Indonesian Physical Review
Volume 09 Issue 02, May 2026
P-ISSN: 2615-1278, E-ISSN: 2614-7904

Identification of Groundwater Potential in Manokwari Formation in Amban Village, Manokwari, West Papua Using Vertical Electrical Sounding 1-D

Ceni Febi Kurnia Sari[1*], Anik Hilyah[2], Ishak S. Erari[3], Fajar K. Rohmala[4], Yoszi Mingsi Anaperta [5]

[1] *Department of Mining Engineering, Faculty of Mining and Petroleum Engineering, Universitas Papua, Manokwari, Papua Barat 98314, Indonesia*
[2] *Department of Geophysical Engineering, Faculty of Civil Engineering, Planning and Geo Engineering, Institut Teknologi Sepuluh Nopember, Sukolilo, Surabaya 60111, Indonesia*
[3] *Department of Physics, Faculty of Mathematics and Natural Sciences, Universitas Papua, Manokwari, Papua Barat 98314, Indonesia*
[4] *Department of Environmental Engineering, Faculty of Civil Engineering and Planning, Institut Teknologi Adhi Tama Surabaya, Surabaya 60117, Indonesia*
[5] *Department of Mining Engineering, Faculty of Engineering, Universitas Negeri Padang, Padang, Sumatra Barat 25131, Indonesia*

Corresponding Author's E-mail: c.sari@unipa.ac.id

Article Info

Article info:
Received: 16-09-2025
Revised: 09-03-2026
Accepted: 13-04-2026

Keywords:
VES Geoelectric; Resistivity; Groundwater; Limestone; Aquifer

How To Cite:
C. F. K. Sari, A. Hilyah, I. S. Erari, F. K. Rohmala, and Y. M. Anaperta, "Identification of Groundwater Potential in Manokwari Formation in Amban Village, Manokwari, West Papua Using Vertical Electrical Sounding 1-D", Indonesian Physical Review, vol. 9, no. 2, p 248-268, 2026.

DOI:
https://doi.org/10.29303/ipr.9i2.576.

Abstract

Amban Village (Manokwari, West Papua) has promising groundwater potential, but it is underutilized due to the complex hydrogeology of Quaternary karst limestone, which features rapid fracture conduit flow, low surface permeability, and seasonal water scarcity. This study mapped subsurface aquifers using 1-D Vertical Electrical Sounding (VES; Schlumberger) at nine stations (ST1–ST9) near high-demand areas. Data were collected with an MAE C313-SEV meter (AB/2 = 1–60 m; ~120 m depth) and inverted in IP2WIN, yielding 8–11-layer models with RMS errors of 4.82–24.80%. Conductive layers interpreted as aquifers (0.3–1059 Ω·m) occur at ST4–ST5 (26–30 m; 1–27 Ω·m), ST9 (23–47 m), shallow zones at ST6–ST8 (4–9 m), and deeper targets at ST1–ST2 (43–64 m), generally beneath a resistive cover that helps protect water quality and sustain yield. The observed resistivity-depth patterns indicate both free (unconfined) and confined aquifer systems typical of karst limestone environments. These findings provide a robust scientific foundation for identifying optimal well-drilling locations and developing sustainable groundwater management strategies in similar karst limestone regions. Pump testing and borehole drilling are strongly recommended to confirm aquifer productivity and hydraulic properties.

Introduction

Water is one of the most essential natural resources for human life, covering the needs of drinking water, households, agriculture, and industry [1], [2], [3]. The increasing population and regional development are often not matched by the availability of adequate clean water, leading communities to rely on groundwater as a primary source, increasingly [4], [5]. However, the availability of groundwater varies across regions, as it is strongly influenced by local geological and hydrogeological conditions, such as rock type (lithology), geological structure, and topography [4], [5], [6].

Amban Village is one of the regions facing challenges in meeting clean water demands, especially during the dry season. One of the main factors suspected to contribute to water scarcity in this area is the lithological condition, which is dominated by Quaternary-aged limestone consisting of coral limestone and calcirudite [7]. Areas with limestone lithology are often recognized as karst regions, which possess unique and complex hydrological characteristics [8], [9]. Limestone, as a rock that easily dissolves in rainwater, forms distinct karst morphology, such as hills, circular valleys (dolina), cave systems, and underground river networks [9]. This dissolution process creates fractures and integrated conduits beneath the surface [8].

Although capable of storing water supplies for about 25% of the world's population [8], the karst hydrological system faces several challenges, such as water flow tending to be concentrated in underground networks [9], low permeability outside the fracture zones [6]. This system is vulnerable to drought because water quickly flows into it, causing the surface to dry out rapidly and reducing spring flows during dry seasons. This condition has been observed in various limestone regions in Indonesia, such as in South Aceh Regency, where there is difficulty exploring water up to a depth of 200 meters in underground caves [9], and in the coastal areas of Malang Regency, where groundwater flow is concentrated in sub-surface conduits, causing droughts during the dry season[8].

Given the challenges posed by limestone lithology, a specialized approach is necessary to identify potential groundwater sources. Geophysical methods, such as electrical resistivity, have become an effective solution to map sub-surface structures, identify the presence of cavities (caves) filled with water, and detect underground river flow paths without the need for expensive and risky drilling[1], [2], [3], [8], [9], [10], [11]. This method is suitable because it can detect subsurface layers and reduce drilling costs [9]. It utilizes the resistivity differences in rocks to study subsurface geology. Each rock type has a different resistivity, so resistivity profiles can identify subsurface structural layers and detect groundwater [12].

Several studies have successfully used various geophysical methods to identify groundwater potential under different geological conditions, including the Wenner [5], Dipole-Dipole [13], and Pole-Pole methods, which are suitable for deep sedimentary rock layers [9], as well as the Wenner-Schlumberger combination [10]. Among these configurations, the Schlumberger configuration is the most frequently used because it is considered adequate for groundwater studies [3], [11], [12], [13], [14], [15], [16]. Specifically, to determine the vertical characteristics of rock layers at a point, the Vertical Electrical Sounding (VES) technique is the primary choice because this method is very effective for determining variations in resistivity values, thickness, and depth of each subsurface rock layer [3], [9], [14], [17]. This study will use the VES technique with the Schlumberger electrode configuration, which has been shown to be reliable in various studies for groundwater exploration [3], [12], [15], [16], [18]. This research offers novelty by

focusing on mapping groundwater potential in Amban Village, which features specific lithological characteristics in the form of Quaternary limestone (reef limestone and calcirudite), which have not been thoroughly identified before. By applying the vertical electrical sounding (VES) technique with a Schlumberger configuration, this study effectively dissects the complexity of the karst hydrological system in the area, addressing the challenge of low permeability outside fracture zones. By accurately identifying aquifer depth and distribution, this research provides strategic solutions for determining optimal drilling locations while minimizing the risk of exploration failure in unpredictable subsurface structures.

Geological Setting

The Manokwari Basin is located to the northeast of the Bird's Head Peninsula, West Papua, with hilly terrain rising to 350 meters above sea level [19]. To the west, there is a coastal plain dominated by Quaternary sediments to the north of the Sorong Fault. This region has experienced compressional deformation from the late Pliocene to the Pleistocene, uplifting and folding the upper Miocene to lower Pliocene sediment succession [19].

The main stratigraphy of this area includes several key formations. The basement rocks are not exposed, but along the Arfak Mountains, there are Arfak Volcanic Rocks from the Oligocene [20], which are conformably overlain by the Maruni Limestone Formation (lower to middle Miocene) [19]. The Maruni Formation is exposed in two anticlines that form a ridge approximately 15 km southwest of Manokwari. Above this, there is the Befoor Formation (upper Miocene to lower Pliocene), which consists of poorly sorted sandstone. The youngest formation is the Manokwari Formation [20], consisting of coral reefs and coral deposits around Manokwari and the coast extending to Oransbari, indicating ongoing tectonic uplift [21]. Additionally, there are alluvial, littoral, and landslide debris deposits scattered across the region [19].

Research Methods

From an administrative perspective, the research is situated in Amban Village, which is part of the West Manokwari Subdistrict within the Manokwari Regency of the West Papua Province. The research concentrated on areas with high population density, specifically the vicinity of the University of Papua. The selection of data points was based on the following parameters: accessibility within 90 meters; avoidance of swamps and lakes; avoidance of highways or public roads (to mitigate potential hazards to local community activities); and location on vacant land in proximity to housing. The present study was conducted at nine measurement points, as illustrated in Figure 2. A comprehensive study was conducted to collect resistivity geoelectric data. This study was conducted to gather information on the subsurface structure, including sediment layer thicknesses and their boundaries with bedrock layers. Additionally, the study aimed to identify water-saturated layers within the designated study area.

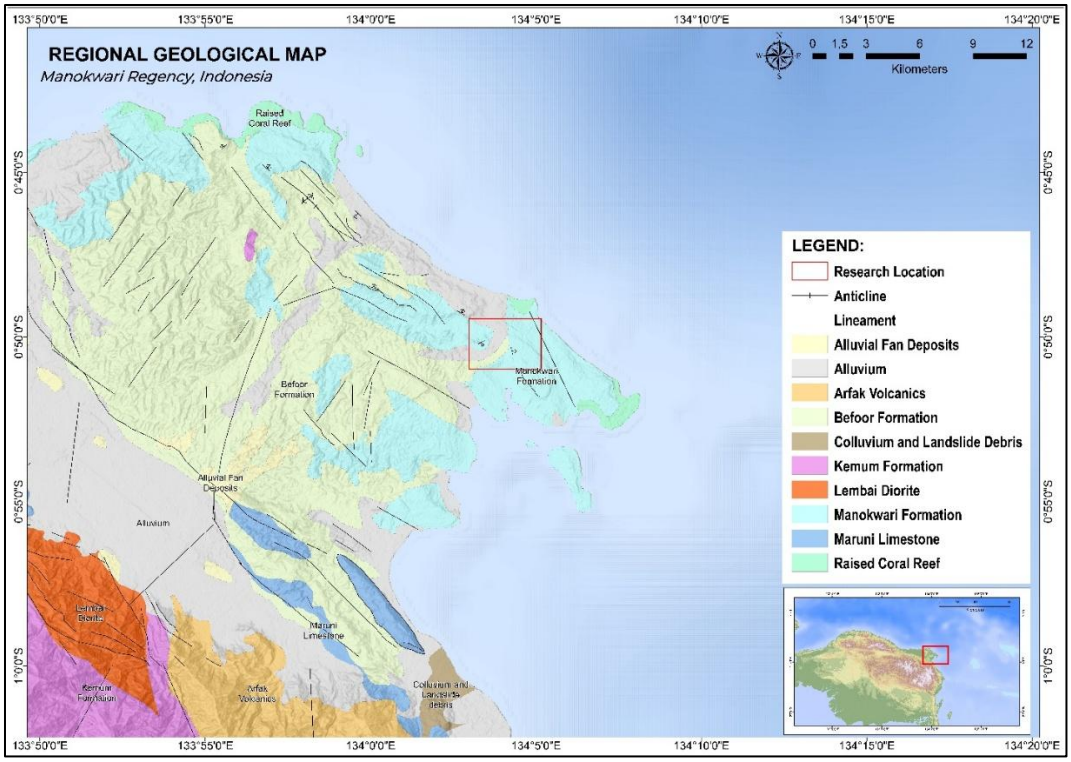

Figure 1. Regional geological map of the Manokwari sheet [20]. The research area is indicated by a red box, comprising fan alluvium deposits, alluvium, and the Manokwari Formation.

A direct current resistivity survey was conducted using a 1-D Vertical Electrical Sounding (VES) approach to investigate vertical variations in subsurface resistivity at nine sounding stations (ST-1 to ST-9), each trajectory has a length of 100-150 meters. Station locations are shown in Figure 2, and data collection photographs are shown in Figure 3. Data were acquired using a Schlumberger electrode configuration, where AB are the current electrodes, and MN are the potential electrodes. For each VES station, the current electrode half-spacing AB/2 was progressively increased from 1 to 60 m (i.e., AB = 2–120 m), while the potential electrode spacing (MN) was kept constant at 1–30 m.

The Schlumberger electrode configuration approach is applied for Vertical Electricity Sounding (VES). In the Schlumberger configuration, the current electrodes (C1 and C2) are positioned at a significantly greater distance compared to the potential electrodes (P1 and P2). A MAE C313-SEV georesistivity meter equipped with four electrodes was utilized in the performance of VES measurements with a 1-D Schlumberger configuration. This research employs the resistivity geoelectric method using the Schlumberger electrode configuration to determine the resistivity of subsurface rocks by applying mathematical equations specific to the configuration. In the Schlumberger configuration, the apparent resistivity equation applied is [22]:

$$\rho_{as} = \frac{k_s \Delta V}{I}; k_s = \frac{\pi(s^2 - a^2)}{4a} \quad (1)$$

In the context of Schlumberger configuration VES, the distance AB increases logarithmically, with the results plotted as a function of the logarithm of apparent resistivity versus the logarithm

of AB/2. Subsequently, the data are analyzed to facilitate recovery of the 1-D resistivity structure, defined as a series of layer thicknesses and resistivities that correspond to the measured response. Conventionally, 1-D sounding data use a curve type, in which

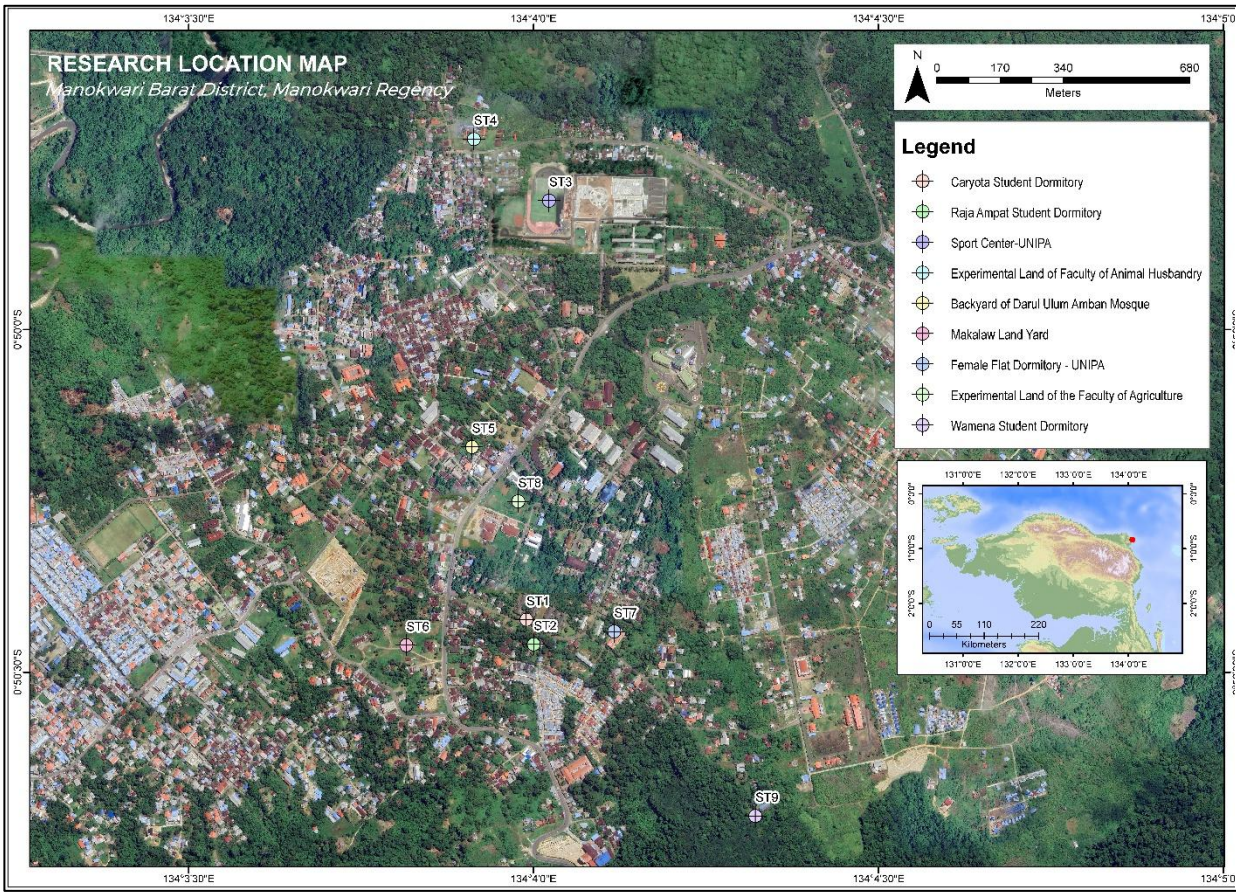

Figure 2. Resistivity Geoelectric Research Location to Identify Groundwater Potential in Amban Village, Manokwari Regency.

the inversion process involves manually adjusting the observed response (sounding curve) to align with a series of theoretical responses. The analysis of the 1-D VES data was performed using the complementary software IP2WIN, which employed forward and inverse modeling. The apparent resistivity dataset for each sounding point (log ρa vs log AB/2) was imported into IP2WIN. The initial model was generated automatically (auto-initial model option), and the inversion iteratively adjusted the 1-D layered-earth parameters (layer resistivity and thickness) to minimize the misfit between observed and calculated curves. The final model was selected based on the minimum RMS error, while also ensuring the calculated curve follows the overall trend of the measured data.

Figure 3. 1-D VES resistivity data measurement at Station I (ST-1). The AB spread ranges from 2 to 120 m, and the MN range is 1-40 m.

Result and Discussion

Forward and inverse modeling were carried out for nine sounding points using Vertical Electrical Sounding (VES) data in the form of apparent resistivity values of subsurface rocks. Field curves were interpreted using forward modeling and 1-D inversion in IP2WIN, yielding a layered earth model with 8–11 layers per station. Overall model fit was acceptable for first-order hydrogeological interpretation, with RMS mismatches ranging from 4.82% to 24.80%. Most stations exhibited low to moderate RMS values (e.g., ST-5 = 4.82%, ST-4 = 5.84%, ST-2 = 6.60%, ST-8 = 6.43%), while station 7 (ST-7) exhibited the highest RMS error of 24.80%, which was significantly higher than those of the other stations. This high discrepancy indicates strong lateral heterogeneity or interference during data acquisition; therefore, the interpretation at this point should be regarded with low confidence and requires further validation. A summary of key parameters for all stations is presented in Table 1.

Table 1. Summary of 1-D VES inversion (IP2WIN)

Station	No. of layers	RMS (%)	Resistivity range, ρ (Ω m)	Interpreted aquifer layer(s) (model)	Aquifer depth (m bgs)	Aquifer resistivity, ρ (Ω m)
ST-1	11	13.20	0.276–291	Layer 11	>64.4	0.276
ST-2	8	6.60	0.609–1374	Layer 7	~43.8	8.08
ST-3	11	7.70	149–47,496	—	—	—
ST-4	9	5.84	1.13–1721	Layer 8 (and possibly Layer 9)	~26.8	1.13 (Layer 8); 4.68 (Layer 9)
ST-5	9	4.82	27–1185	Layer 8 (and possibly Layer 9)	~30.5	27 (Layer 8); 35.9 (Layer 9)
ST-6	8	7.73	12.7–10,507	Layer 5	~3.58	12.7
ST-7	11	24.80	10.8–8,291	Layers 6–7	~6.32–8.51	10.8–19.2
ST-8	10	6.43	0.0014–1267	Layers 5–6	~4–9	0.0014–3.01
ST-9	10	7.95	123–3655	Layers 8–9	~23–47	262–1059

At station 1 (ST-1), vertical electrical sounding (VES) modeling revealed variations in subsurface resistivity, divided into 11 layers, with an average root-mean-square (RMS) value of 13.20%. This RMS value indicates the level of discrepancy between the measurement data and the model, yet it remains within the tolerance limits for initial interpretation (Figure 4). The layer parameter table demonstrates a range of resistivity (ρ) values from 113 Ω.m to 0.276 Ω.m, with increasing thickness (d) and cumulative depth (Alt). The layers between 1 and 5 exhibit relatively high resistivity (113-291 Ω.m), suggesting the presence of sandy material or consolidated rock. A substantial decrease in resistivity is observed in layers 6 to 10 (5.54-64.4 Ω.m), with a subsequent rise in resistivity in layer 11 (0.276 Ω.m). The apparent resistivity curve as a function of AB/2 electrode spacing shows a decreasing trend in resistivity with increasing AB/2 spacing, indicating the presence of conductive layers at depths greater than 20 meters. A substantial decrease in resistivity at AB/2 distances greater than 100 meters (less than 1 Ω.m) lends further credence to the hypothesis of a water-saturated zone (aquifer) in the deepest layers.

The interpretation of the subsurface layers at ST-1 is related to resistivity variations and local geological configurations. The layers between 1 and 5 (ranging in depth from 0 to 8.6 meters) are believed to be linked to dry sand or limestone, as indicated by their high resistivity levels (>100 Ω.m). The layers between 6 and 10 (ranging in depth from 8.6 to 64.4 meters) exhibited a decline in resistivity (ranging from 5.54 to 64.4 Ω.m), suggesting a transition to clay or clayey sand with elevated porosity. The low resistivity of layer 11 (0.276 Ω.m) at depths>64.4 meters indicates a confined aquifer with substantial groundwater content. The relatively high RMS value of 13.20% may be attributed to subsurface heterogeneity or noise during data acquisition. However, the consistency of the decreasing resistivity trend in the VES curve and the deepest conductive layer supports the validity of the model.

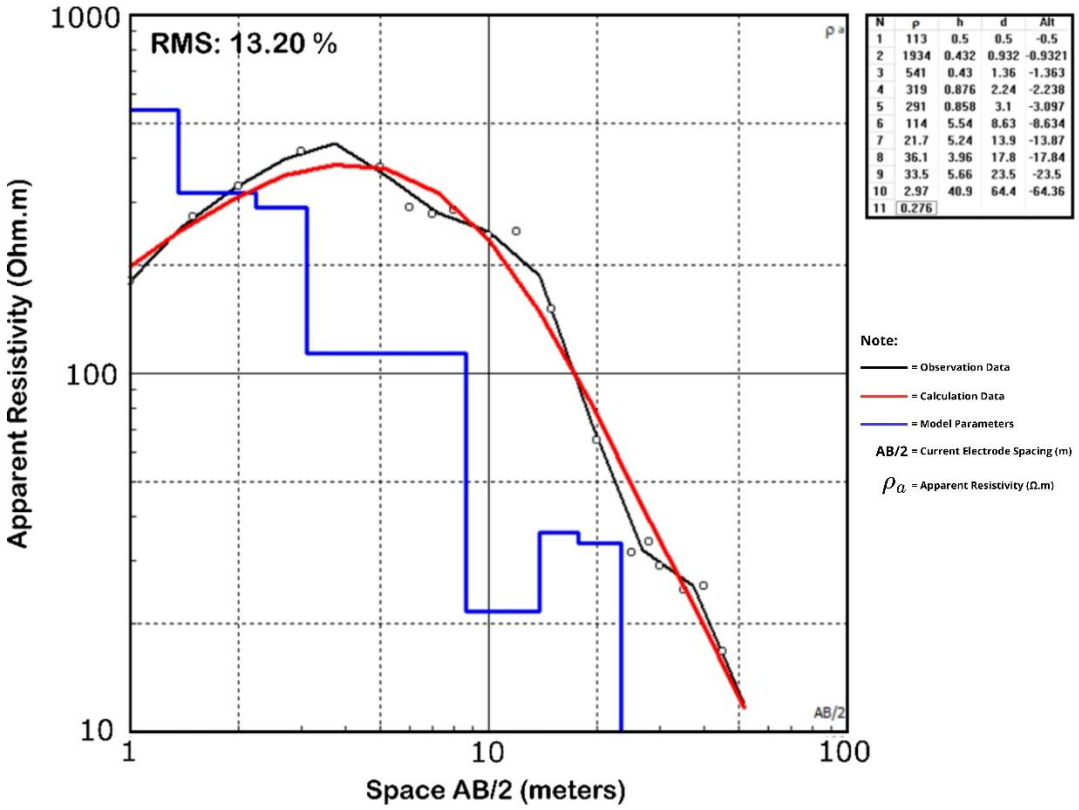

Figure 4. Inversion results of 1-D VES resistivity data at Station I (ST-1), showing the distribution of observation data points (open circles) and their trend (black curve). The red curve shows the calculated data from the inversion process, with an RMS error of 13.20%, while the blue staircase line shows the 1-D model parameters (true resistivity vs. depth).

Station two (ST-2) revealed a subsurface structure divided into eight layers with an RMS value of 6.60%, indicating a higher degree of agreement between the measurement data and the model than at ST-1 (Figure 5). The layer parameter table indicates a variation in resistivity (ρ) ranging from 0.609 Ω.m to 1374 Ω.m, accompanied by a substantial increase in thickness (h) and cumulative depth (Alt). The layers between 1 and 4 exhibit low to medium resistivities (0.609-4.61 Ω.m), suggesting the presence of wet clay or clayey sand. An extreme resistivity spike is observed in layer 5 (1374 Ω.m), This finding suggests the presence of hard rock or dry gravel. Subsequently, resistivity declines in layers 6-7 (107-8.08 Ω.m), followed by an increase

in layer 8 (34.5 Ω.m). It should be noted, however, that data pertaining to layer 8 is incomplete. The apparent resistivity curve against electrode spacing exhibits a fluctuating pattern, characterized by a decrease in resistivity at a distance of AB/2 less than 10 meters, followed by a sharp increase at AB/2 around 10-40 meters, and a subsequent decrease at AB/2 more than 40 meters. This phenomenon indicates the complexity of the subsurface structure, with the potential presence of a conductive layer (aquifer) at a depth of more than 43 meters (layer 7).

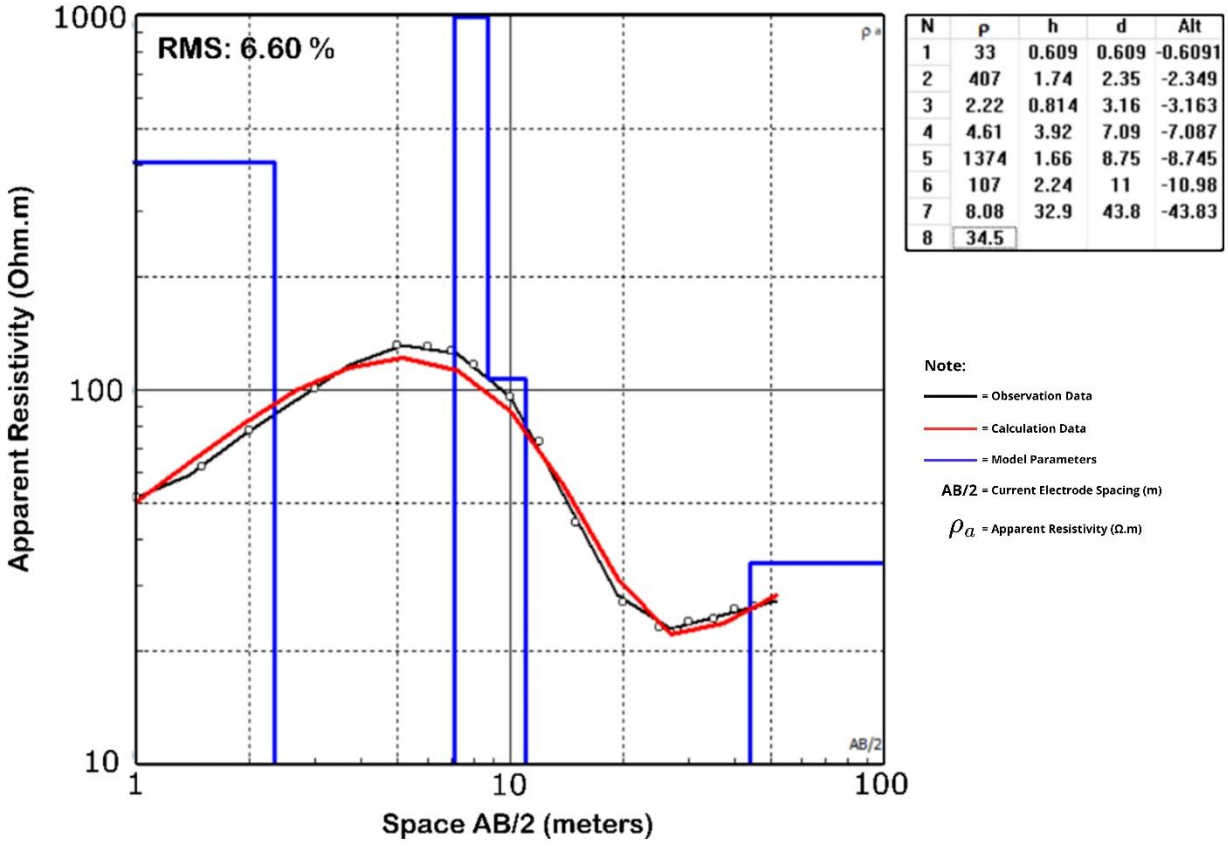

Figure 5. Inversion results of 1-D VES resistivity data at Station II (ST-2), showing the distribution of observation data points (open circles) and their trend (black curve). The red curve shows the calculated data from the inversion process, with an RMS error of 6.60%, while the blue staircase line shows the 1-D model parameters (true resistivity vs. depth).

The presence of resistivity variations in layers 1-4 (0-7.09 meters) indicates clayey sedimentary material or clayey sand affected by surface water. The resistivity spike in layer 5 (1374 Ω.m, 8.75 meters deep) can be interpreted as an indication of fragmented volcanic rocks or of impermeable dry gravel layers. The observed decrease in resistivity within layers 6-7 (107-8.08 Ω.m) suggests the potential presence of a transition zone, indicating a shift to materials with high porosity, such as sand or volcanic breccia, which may be filled with water. The resistivity of 8.08 Ω.m in layer 7, located at a depth of 43.8 meters, indicates a deep aquifer with substantial groundwater content. The lower root-mean-square (RMS) value of 6.60%

compared with ST-1 indicates enhanced model precision, which may be attributable to relatively homogeneous subsurface conditions or optimized inversion methodologies. However, incomplete data in layer 8 (34.5 Ω.m) introduces uncertainty regarding the structure at depths greater than 43.8 meters.

Furthermore, the VES modeling results at station three (ST-3) reveal a subsurface structure comprising 11 layers, with an RMS value of 7.70%, indicating a moderate fit between the measured data and the model (Figure 6). The layer parameter table shows significant variations in resistivity (ρ), ranging from 149 Ω.m to 47,496 Ω.m, with a cumulative depth of up to 67.83 meters. Layers 1–10 exhibit medium to high resistivity (149–2921 Ω.m), likely dominated by sandy, gravelly, or consolidated rock materials. An observed increase in resistivity in layer 11 (47,496 Ω.m) may indicate hard, non-porous rock or geological anomalies, such as granite intrusions. The apparent resistivity curve against the electrode distance AB/2 shows a trend strongly influenced by layer 11, with the possibility of a sharp resistivity increase at depths exceeding 67 meters. Consistent AB/2 measurements at 100 meters indicate a focus on exploring the inner zone, although the uniformity of this distance needs to be re-evaluated to ensure data validity.

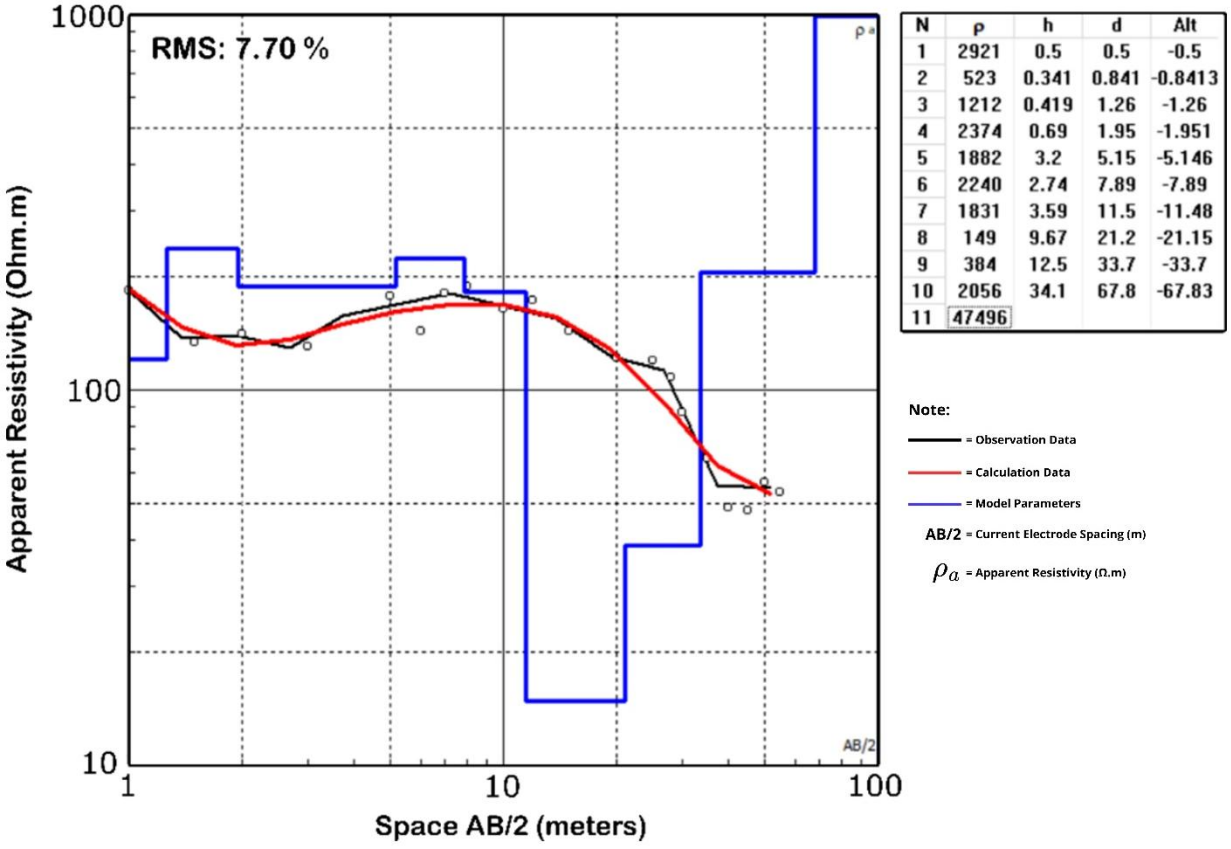

Figure 6. Inversion results of 1-D VES resistivity data at Station III (ST-3), showing the distribution of observation data points (open circles) and their trend (black curve). The red curve shows the calculated data from the inversion process, with an RMS error of 7.70%, while the blue staircase line shows the 1-D model parameters (true resistivity vs. depth).

The variation in resistivity within layers 1–10 (0–67 meters) indicates characteristics of dry to semi-consolidated sediment materials, such as sand, gravel, or fragmented volcanic rock. The resistivity of 47.496 Ω.m in layer 11 is an unusually high value in hydrogeological contexts, raising two possibilities: (1) the presence of massive impermeable bedrock (e.g., granite, metamorphic rock), or (2) inversion artifacts due to limitations in model resolution at extreme depths. If valid, this layer could act as a natural barrier to groundwater flow, confining the aquifer to shallow zones. An RMS value of 7.70% indicates model uncertainty due to subsurface heterogeneity or disturbances during data acquisition. The consistency of the AB/2 distance at 100 meters also needs to be considered, as variations in distance are generally required to achieve optimal vertical resolution. The fluctuating resistivity pattern in layers 1–10 may reflect a complex geological structure, such as volcanic rock layering or faulting.

The VES modeling results at the fourth station (ST-4) reveal a subsurface structure comprising 9 layers, with an RMS value of 5.84%, indicating a very good fit between the measured data and the model (Figure 7). The layer parameters table shows a resistivity (ρ) variation from 1.13 Ω.m to 1721 Ω.m, with a cumulative depth of 26.84 meters. Layers 1 to 7 are dominated by medium to high resistivity (281–1721 Ω.m), which is suspected to be related to dry sandy material, gravel, or fragmented volcanic rock. An extreme decrease in resistivity occurs at layer 8 (1.13 Ω.m), followed by a moderate increase at layer 9 (4.68 Ω.m), although the thickness data for layer 9 is incomplete. The apparent resistivity curve versus electrode distance AB/2 (Figure 7) shows a fluctuating trend with a resistivity range of 1–1000 Ω.m. The decrease in resistivity at a certain AB/2 distance indicates the presence of a conductive layer at a depth of more than 12 meters (layer 8), while an increase in resistivity at a certain spacing may be associated with shallow resistive layers (layers 2 and 6).

The resistivity variations in layers 1-7 (0-12.3 meters) indicate the characteristics of dry sedimentary materials or semi-consolidated volcanic rocks. The high resistivity detected in layers 2 (1431 Ω.m) and 6 (1283 Ω.m) can be interpreted as zones of dry gravel or resistive rocks that function as barriers to water flow. The drastic decrease in resistivity in layer 8 (1.13 Ω.m) at 26.8-meter depth is a strong indication of a water-saturated zone (aquifer) with high porosity, possibly in the form of sand or volcanic breccia filled with water. The higher but still low resistivity in layer 9 (4.68 Ω.m) indicates a possible transition to clay material or a confined aquifer with low salinity. The low RMS value of 5.84% indicates a high level of model accuracy, supported by the consistency of the VES curve trends. However, the incompleteness of layer 9 thickness data and fluctuations in the apparent resistivity curve raise questions regarding subsurface heterogeneity or potential interference during data acquisition.

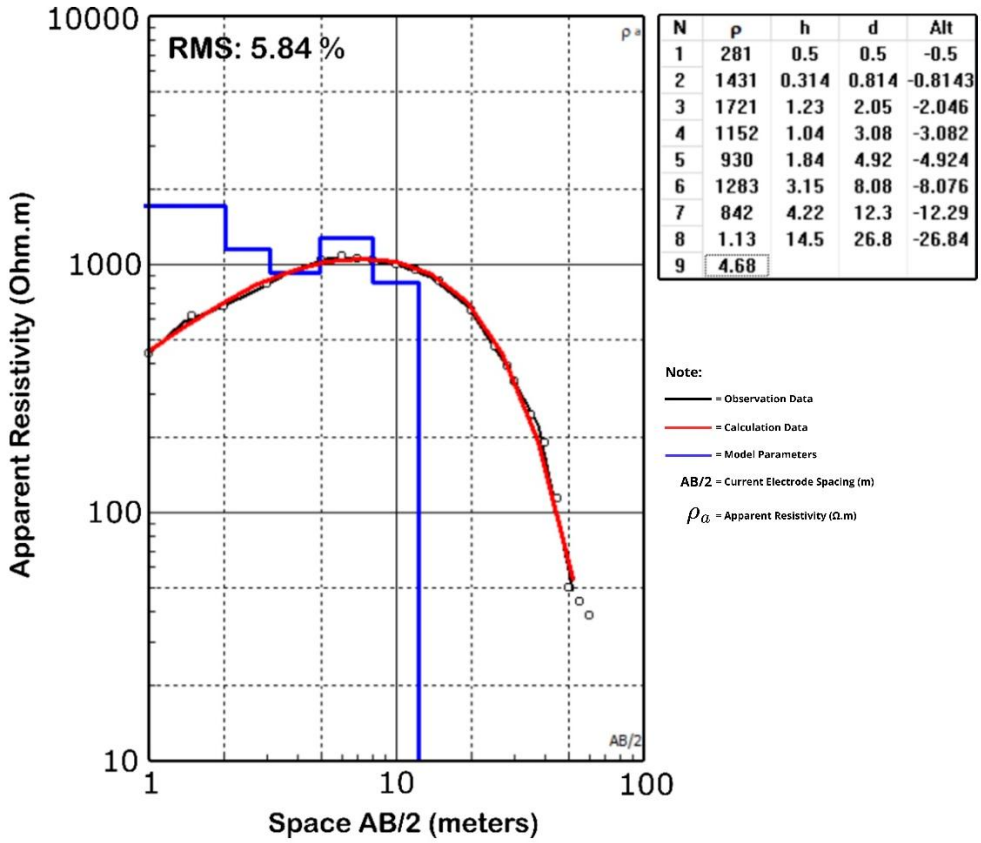

Figure 7. Inversion results of 1-D VES resistivity data at station IV (ST-4), showing the distribution of observation data points (open circles) and their trend (black curve). The red curve shows the calculated data from the inversion process, with an RMS error of 5.80%, while the blue staircase line shows the 1-D model parameters (true resistivity vs. depth).

The VES modeling results at the fifth station (ST-5) yield a subsurface structure divided into 9 layers, with an RMS value of 4.82%, indicating excellent agreement between the measured data and the model (Figure 8). The layer parameter table shows a variation in resistivity (p) from 27 Ω.m to 1185 Ω.m, with a cumulative depth of 30.52 meters. Layers 1-4 have high resistivity (694-1185 Ω.m) and are dominated by dry, sandy material or consolidated volcanic rock. A gradual decrease in resistivity is observed in layers 5-8 (348-27 Ω.m), with the lowest value in layer 8 (27 Ω.m), suggesting a conductive zone. The resistivity of layer 9 (35.9 Ω.m) shows a moderate increase, although the thickness and depth data are incomplete. The apparent resistivity curve against AB/2 electrode spacing shows consistent measurements at AB/2 100 meters, emphasizing the importance of focusing exploration on the deep zone. The decrease in resistivity in layers 5-8 aligns with this acquisition trend, while fluctuations in layer 9 require further analysis.

The resistivity variations in layers 1-4 (0-2.25 meters) indicate the resistive characteristics of dry sedimentary materials or volcanic rocks, which could potentially function as impermeable layers. The decrease in resistivity in layers 5-8 (4.14-30.52 meters deep) indicates a transition to materials with high porosity, such as sand or volcanic breccia, both of which are water-filled. The resistivity of 27 Ω.m in layer 8 (30.5 meters depth) is a strong indicator of a water-

saturated zone (aquifer) with low salinity. The increase in resistivity in layer 9 (35.90 Ω.m) may indicate clay or a transition to a confined aquifer with lower water content. The low RMS value of 4.82% indicates high model accuracy, supported by the consistency of the AB/2 measurement data. However, incomplete data in layer 9 and the uniformity of the AB/2 spacing at only 100 meters may limit the resolution of shallow-layer interpretation. The fluctuating resistivity pattern may also reflect local heterogeneity, such as faulting or rock intrusion.

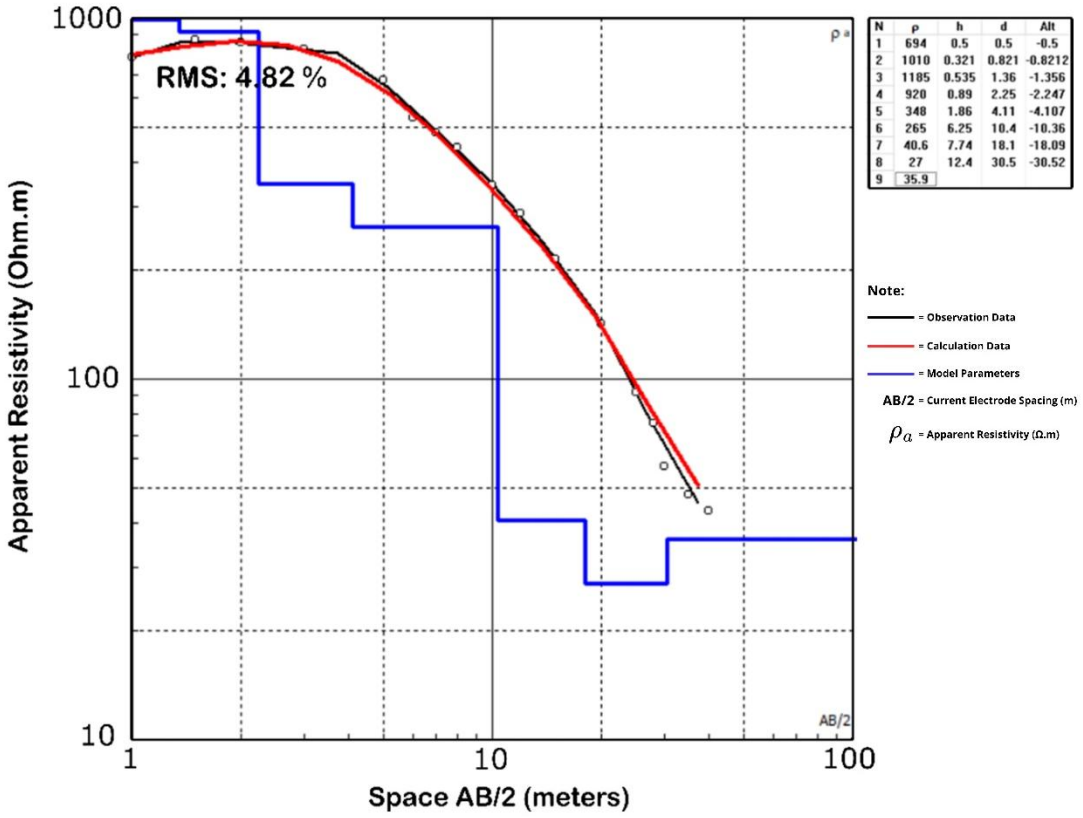

Figure 8. Inversion results of 1-D VES resistivity data at Station V (ST-5), showing the distribution of observation data points (open circles) and their trend (black curve). The red curve shows the calculated data from the inversion process, with an RMS error of 4.82%, while the blue staircase line shows the 1-D model parameters (true resistivity vs. depth).

The VES modeling results of station six (ST-6) provide a subsurface structure divided into eight layers with a Root Mean Square (RMS) value of 7.73%, indicating a moderate agreement between the measurement data and the model. The resistivity (ρ) ranges from 12.7 Ω.m to 10,507 Ω.m, with a cumulative depth of 21.27 meters. Layers 1-4 have intermediate resistivities (88.4-46.1 Ω.m), which are thought to consist of clayey sand or altered volcanic rock. A drastic decrease in resistivity in layer 5 (12.7 Ω.m) indicates the presence of a conductive zone, followed by an increase in layers 6-7 (33.8-13 Ω.m). The extreme spike in layer 8 (10,507 Ω.m) is striking and warrants further investigation. The apparent resistivity curve versus electrode spacing AB/2 (Figure 9) shows a fluctuating pattern with a range of 10-1000 Ω.m. The decrease

in resistivity at AB/2 of 10-100 meters corresponds to the presence of conductive layers (layers 5-7), while the resistivity spike in layer 8 may be detected at larger AB/2 spacing.

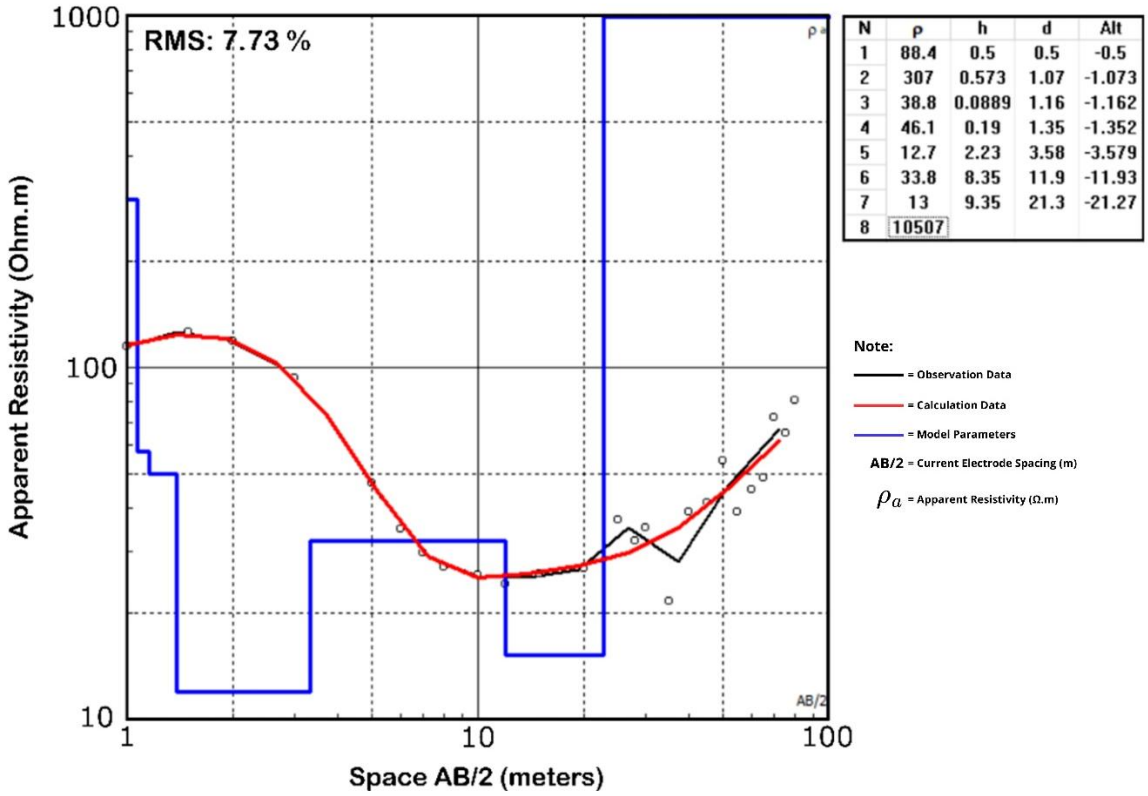

Figure 9. Inversion results of 1-D VES resistivity data at Station VI (ST-6), showing the distribution of observation data points (open circles) and their trend (black curve). The red curve shows the calculated data from the inversion process, with an RMS error of 7.73%, while the blue staircase line shows the 1-D model parameters (true resistivity vs. depth).

Layers 1-4 (0-1.35 meters) are interpreted as dry sedimentary material or semi-consolidated volcanic rock with low porosity. The low resistivity in layer 5 (12.7 Ω.m, 3.58 meters depth) indicates a water-saturated zone (shallow aquifer) with wet clay or sand material. The increase in resistivity in layers 6-7 (33.8-13 Ω.m) may reflect local heterogeneity, such as rock intrusion or transition to medium porosity materials. The extreme resistivity spike in layer 8 (10,507 Ω.m) at 21.27-meter depth is very unusual in a hydrogeological context. Possible interpretations include: Impermeable massive bedrock (e.g., granite, metamorphic rocks), inversion artifacts due to model resolution limitations at extreme depths, or geological anomalies (e.g., igneous intrusions or mineralization). The moderate RMS value of 7.73% indicates the presence of subsurface heterogeneity or noise during data acquisition. The limited AB/2 spacing (10-100 meters) may also reduce the resolution of deep layers.

The VES modeling results at station 7 (ST-7) provide a subsurface layer structure divided into 11 layers with an RMS value of 24.80%, indicating a significant discrepancy between the measured and modeled data (Figure 10). The layer parameter table shows extreme variations in resistivity (p), ranging from 10.8 Ω.m to 8,291 Ω.m, with a cumulative depth of 42.4 meters.

Layers 1-5 have high resistivity (93.3-2581 Ω.m), dominated by resistive materials such as dry sand or consolidated volcanic rock. A drastic decrease in resistivity in layers 6-7 (19.2-10.8 Ω.m) indicates the presence of conductive zones, followed by a gradual increase in layers 8-10 (47.6-713 Ω.m). The extreme spike in layer 11 (8,291 Ω.m) is striking and warrants an in-depth investigation. The apparent resistivity curve versus AB/2 electrode spacing shows inconsistencies, in line with the high RMS values. Extreme fluctuations in the range of 10-1000 Ω.m may reflect subsurface heterogeneity or noise during data acquisition.

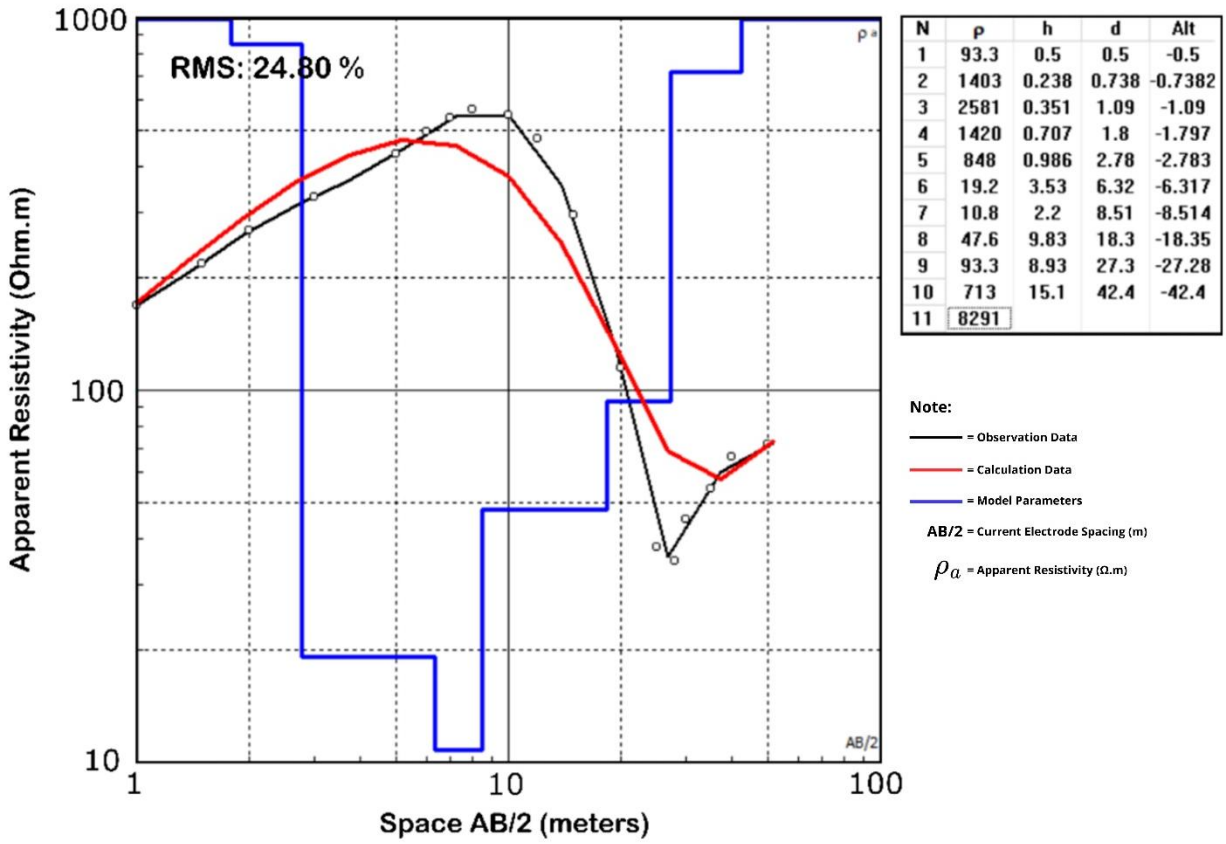

N	ρ	h	d	Alt
1	93.3	0.5	0.5	-0.5
2	1403	0.238	0.738	-0.7382
3	2581	0.351	1.09	-1.09
4	1420	0.707	1.8	-1.797
5	848	0.986	2.78	-2.783
6	19.2	3.53	6.32	-6.317
7	10.8	2.2	8.51	-8.514
8	47.6	9.83	18.3	-18.35
9	93.3	8.93	27.3	-27.28
10	713	15.1	42.4	-42.4
11	8291			

Figure 10. Inversion results of 1-D VES resistivity data at Station VII (ST-7), showing the distribution of observation data points (open circles) and their trend (black curve). The red curve shows the calculated data from the inversion process, with an RMS error of 24.80%, while the blue staircase line shows the 1-D model parameters (true resistivity vs. depth).

The high RMS value of 24.80% indicates the model's inaccuracy, caused by: 1. Complex geological heterogeneity, such as discontinuous volcanic rock layers or fault structures. 2. Noise during data acquisition, such as electromagnetic interference or poor electrode contact. 3. Limitations of inversion resolution in handling extreme resistivity variations. Layers 1-5 (0-2.78 meters): Resistive material (dry sand, volcanic rock) with low porosity. Layers 6-7 (6.32-8.51 meters): Low resistivity (10.8-19.2 Ω.m) indicates a water-saturated zone (shallow aquifer) with clay or wet sand. Layers 8-10 (18.3-42.4 meters): Resistivity increases (47.6-713 Ω.m), presumably transition to semi-consolidated rock or partial impermeable zone. Layer 11 (>42.4 meters): Extreme 8,291 Ω.m resistivity may represent massive bedrock (granite/metamorphic rock) or inversion artifacts due to extreme depth.

At the eighth measurement station (ST-8), the 1-D geoelectric model derived from the VES measurements showed good agreement between the observed and calculated apparent resistivity data, with an RMS of 6.43%, indicating good model convergence (Figure 11). The model consists of 10 layers with variations in resistivity and thickness that reflect differences in lithology and potential aquifer zones. The fifth layer exhibited an extremely low resistivity (0.0014 Ω·m). In the context of freshwater hydrogeology, this value is too low and is more likely to be interpreted as the influence of very high clay content, saline intrusion, or possibly an inversion artifact. Therefore, this zone cannot be considered a productive freshwater aquifer target without further supporting evidence from drill data. The sixth layer had a very low resistivity (3.01 0-m) with thicknesses of 1.08 m and 4.09 m, indicating water-saturated clay or a depressed aquifer. The top layer has a resistivity of 49.40 m with a thickness of 0.341 m, representing the resistive topsoil. The second layer has a higher resistivity (101) Q-m) and thickness of 0.431 m, consisting of dense sandy material or weathered volcanic ash. The third layer shows a very high resistivity of 1267 0-m with a thickness of 0.507 m, indicating highly resistive material such as dry sand or gravel. Underneath is a layer with lower resistivity (19.5 0-m) to a depth of 1.08 m, indicating clay material or a water-saturated zone. The fifth and sixth layers have very low resistivity (0.0014 Ω-m and 3.01 0-m) with thicknesses of 1.08 m and 4.09 m, indicating water-saturated clay or a confined aquifer. The seventh to ninth layers show increasing resistivity from 36.6 to 73.4 Q-m to a depth of 25 m, possibly consisting of weathered rock or watery sand. The deepest layer (10th) has a resistivity of 70.3 0-m with a thickness of 82.1 m, thought to be compressed bedrock underlying the aquifer system.

Based on the resistivity characteristics and layer thicknesses, it can be concluded that the measurement location is within a layered aquifer system characterized by free and confined aquifers. The presence of a very low resistivity layer at a depth of 4-9 meters indicates a water-saturated layer with potential as a groundwater source. The pattern of resistivity changes alternating between resistive and conductive layers reflects the complex geological setting common in tropical alluvial or volcanic areas. Interpretation of geoelectric results is important to support sustainable groundwater exploration and management. To obtain a comprehensive picture of aquifer geometry and quality, integration with supporting data, such as borehole logs, pumping tests, and groundwater analyses, is required.

Figure 12 shows the results of 1-D geoelectric modeling based on VES data with Schlumberger configuration at the 9th measurement station (ST-9). The inversion curve shows good agreement with the observation data, with an RMS value of 7.95%. The subsurface model consists of 10 layers with significant variations in resistivity (p) and thickness (h). The surface layer has a resistivity of 123 0-m and a thickness of 0.5 m, representing relatively dry topsoil. The second and third layers show very high resistivity (3655 Q-m and 986 Q-m), with thicknesses of 1.15 m and 0.627 m, interpreted as sand or loose material layers. The fourth and fifth layers have lower resistivity (298 2-m and 194 0-m) with thicknesses of 1.65 m and 1.61 m, indicating increased moisture. The sixth and seventh layers show high resistivity (434) Q-m and 2030 Q-m) with thicknesses of 2.53 m and 6.3 m, respectively. The eighth and ninth layers reflect more conductive conditions, with resistivities of 262 and 1059 Q-m and thicknesses of 9.27 m and 8.23 m, respectively. Although layers 8 and 9 in ST-9 exhibited relatively high resistivity values (262–1059 µm), they were still considered potential zones. This is not interpreted as a conductive sedimentary aquifer but rather as a fractured zone in the limestone formation, where groundwater fills secondary cavities within the rock matrix.

The tenth layer has a resistivity of 382 0-m with a thickness of 15.7 m, reflecting compact bedrock.

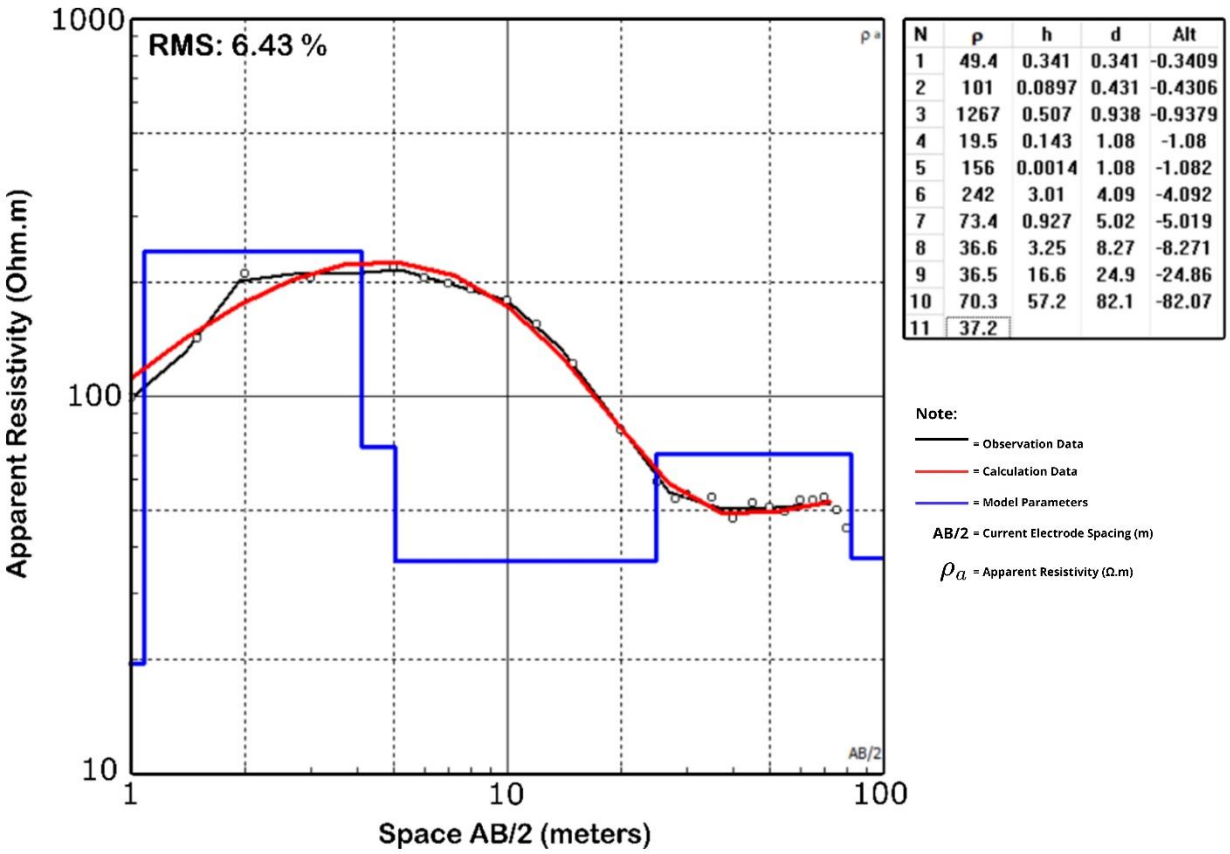

N	ρ	h	d	Alt
1	49.4	0.341	0.341	-0.3409
2	101	0.0897	0.431	-0.4306
3	1267	0.507	0.938	-0.9379
4	19.5	0.143	1.08	-1.08
5	156	0.0014	1.08	-1.082
6	242	3.01	4.09	-4.092
7	73.4	0.927	5.02	-5.019
8	36.6	3.25	8.27	-8.271
9	36.5	16.6	24.9	-24.86
10	70.3	57.2	82.1	-82.07
11	37.2			

Figure 11. Inversion results of 1-D VES resistivity data at Station VIII (ST-8), showing the distribution of observation data points (open circles) and their trend (black curve). The red curve shows the calculated data from the inversion process, with an RMS error of 6.43%, while the blue staircase line shows the 1-D model parameters (true resistivity vs. depth).

The VES results indicate a complex subsurface architecture characterized by alternating resistive and conductive units. The near-surface, high-resistivity layer is interpreted as an unsaturated zone, likely composed of dry sand, gravel, or loosely consolidated rock. Although this horizon is not suitable as a groundwater source, it is significant as a protective cover that helps protect the aquifer. At depths greater than approximately 14 m, the presence of medium- to low-resistivity layers suggests potential aquifer zones. Resistivity values of 262–1059 Ω·m at depths of about 23–47 m are indicative of water-saturated lithologies, ranging from fine sand to saturated silt or water-filled fracture zones. Accordingly, the most prospective groundwater targets occur at medium to deeper levels, where expected productivity is controlled by factors such as lateral continuity and effective porosity. Nevertheless, robust confirmation of aquifer capacity and groundwater quality requires integration with borehole data and pumping tests.

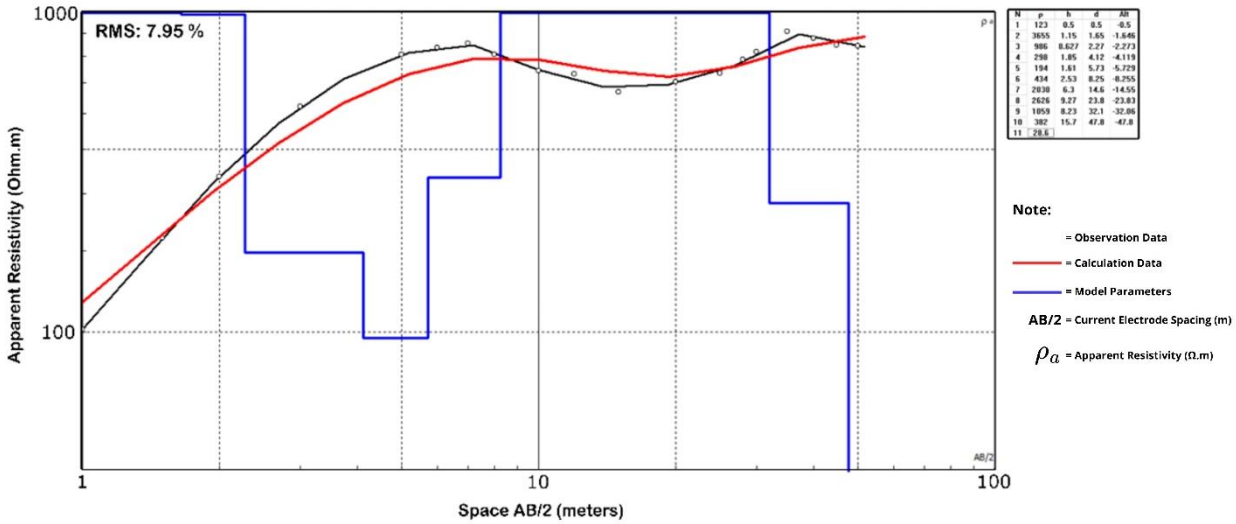

Figure 12. Inversion results of 1-D VES resistivity data at Station IX (ST-9), showing the distribution of observation data points (open circles) and their trend (black curve). The red curve shows the calculated data from the inversion process, with an RMS error of 7.95%, while the blue staircase line shows the 1-D model parameters (true resistivity vs. depth).

The geoelectrical interpretation results from the nine sounding points in the study area show patterns and characteristics that are highly consistent with the principles and findings of various groundwater exploration studies [9], [14], [18], [23], [24], [25]. The dominant signature comprises a resistive shallow layer overlain by a more conductive unit interpreted as an aquifer. Low-resistivity layers identified at ST-1, ST-2, and ST-4 through ST-9 are generally interpreted as aquifer or water-bearing horizons, given that water-saturated rocks typically exhibit higher electrical conductivity [5], [16], [17]. The interpretation of the aquifer lithology as sandstone from the Manokwari and Befoor Formations is strongly supported by several sources stating that sandstone and gravel are common aquifer materials [5], [13], [15], [18], and confirmed by other geoelectrical studies in Manokwari that also identified sandstone as a potential aquifer layer in the same formations [24].

The application of the resistivity geoelectric method, including Vertical Electrical Sounding (VES) with the Schlumberger configuration, is an essential contribution in the field of Earth Physics (Geophysics) because of its ability to map the physical properties of rocks non-invasively [3], [4], [14], [15], [18]. The results of this geoelectrical investigation are highly relevant and practical. By understanding aquifer characteristics in depth using the VES method, it is hoped that optimal well locations can be directly determined, providing an efficient, measurable solution to address clean water availability issues. Moreover, this approach significantly reduces the risk of costly drilling failures and provides a strong scientific foundation for technical planning, making it an effective long-term solution, especially in regions with complex geology, such as the karst of Manokwari.

While 1-D modeling provides a useful vertical representation, it assumes homogeneous lateral layering, which is often not fully realized in complex karst environments. Furthermore, incomplete parameter values in the deepest layers at several stations (e.g., ST-2, ST-4, and ST-5) limit the definition of the aquifer system's lower boundary. Therefore, these interpretations should be used as an initial guide for determining prospective zones. Further validation

through integration with drilling data, lithology logs, and pumping tests is needed to confirm the aquifer's productivity and lateral continuity in the area.

Conclusion

The 1-D Schlumberger VES modeling across nine stations in Amban Village successfully identified subsurface resistivity variations interpreted as potential groundwater-bearing units. The results reveal a complex hydrogeological architecture with significant depth variability, categorized into three distinct zones: shallow (4–9 m at ST-6, ST-7, and ST-8), intermediate (23–47 m at ST-4, ST-5, and ST-9), and deep (>43–64 m at ST-1 and ST-2). Prospective aquifers generally exhibit conductive signatures ranging from 0.3 to 27. However, the interpretation for ST-9 (262–1059) is refined; due to its higher resistivity, it is classified as a water-filled fracture zone within the limestone matrix rather than a typical conductive sediment aquifer. Based on high model convergence and typical freshwater resistivity ranges, ST-4, ST-5, and ST-2 (RMS errors 4.82%–6.60%) are identified as high-priority targets for well development. ST-7 is explicitly flagged as a low-confidence target due to its high RMS error of 24.80%, which suggests significant lateral heterogeneity or noise-related distortions during data acquisition. The extremely low resistivity at ST-8 (0.0014) must be treated with caution; it requires salinity and water-quality verification, as such values may indicate saline influence, high clay content, or represent an inversion artifact rather than a productive freshwater target. Although the VES method provides an effective non-invasive guide for identifying prospective zones, the identified variability and technical uncertainties necessitate further validation. Integration with borehole drilling, lithology logs, and pumping tests is essential to confirm the productivity, water quality, and lateral continuity of these aquifers in the karst environment of Manokwari.

Acknowledgment

The author would like to express sincere gratitude to all colleagues who provided assistance and constructive suggestions throughout this research. In addition, special thanks are extended to the sponsors for their generous financial support.

References

[1] K. Sandeep, A. S. Athira, A. A. Arshak, K. V. Reshma, G. H. Aravind, and M. Reethu, "Geoelectrical and hydrochemical characteristics of a shallow lateritic aquifer in southwestern India," *Geosystems and Geoenvironment*, vol. 2, no. 2, p. 100147, May 2023.

[2] H. M. El-Sayed and A. R. Elgendy, "Geospatial and geophysical insights for groundwater potential zones mapping and aquifer evaluation at Wadi Abu Marzouk in El-Nagila, Egypt," *Egyptian Journal of Aquatic Research*, vol. 50, no. 1, pp. 23–35, Mar. 2024.

[3] B. U. Bukit, M. F. Zakaria, S. B. Kusumayudha, I. Rahatmawati, and T. Setyaningrum, "Pemetaan Muka Air Tanah sebagai Rekomendasi Pengeboran Air Bersih Berdasarkan Data Geolistrik Sounding di Sekitar Embung Batur Agung, Karangmojo, Kabupaten Gunung Kidul," *J. Ilmu Lingk.*, vol. 22, no. 5, pp. 1202–1208, Aug. 2024.

[4] M. D. Erintina, A. S. Ubaidillah, and A. Faesal, "Pemanfaatan Metode Resistivitas Satu Dimensi Untuk Identifikasi Potensi Air Tanah Di Dusun Karang Bayan, Parampuan, Lombok Barat," *JPM*, vol. 3, no. 3, pp. 273–278, Mar. 2024.

[5] A. Iskandar, S. Kamur, and S. Awal, "Analisis Potensi Air Tanah Di Kecamatan Molawe Kabupaten Konawe Utara Menggunakan Geolistrik S-Field Multichanel Metode Wenner," *Jurnal Pendidikan, Sains, Geologi, dan Geofisika (GeoScienceEd Journal)*, vol. 5, no. 3, pp. 732–737, 2024.

[6] F. P. Wambena, A. A. Chandra, and D. A. Rusim, "Identifikasi Kedalaman Muka Air Tanah dan Posisi Akuifer di Kabupaten Tolikara," *jusit*, vol. 2, no. 2, pp. 09–21, Jul. 2024.

[7] B. H. Harahap, B. Sayiful, N. S. Baharuddin H. Penggabean, and T. O. Simanjuntak. 2003. Stratigraphic Lexicon of Indonesia. 1st ed. Bandung, H. Penggabean, and T. O. Simanjuntak, *Stratigraphic Lexicon of Indonesia*, vol. 1. Bandung: The Geological Research and Development Centre, 2003.

[8] A. Wahid, H. L. Sianturi, C. Mbiliyora, and B. Bernandus, "Identifikasi Pola Aliran Akuifer Karst Dengan Metode Geolistrik Self Potensial SP," *fisa*, vol. 9, no. 1, pp. 1–6, Apr. 2024.

[9] A. Amdad, G. Noesanto, F. A. Riyadi, K. J. Saputro, and O. W. Lusantono, "Identifikasi Air Dibawah Batugamping Menggunakan Metode Geolistrik Resistivity 2D Dan Vertical Electrical Sounding Di Kabupaten Aceh Selatan," *Jurnal Teknologi Pertambangan*, vol. 9, no. 2, pp. 100–105, 2024.

[10] R. Lihayati, N. L. Septania, and F. Haroky, "Identifikasi struktur bawah permukaan tanah menggunakan metode geolistrik konfigurasi Wenner-Schlumberger di Kabupaten Rokan Hulu," *Jurnal Pendidikan dan Sains (JUPISI)*, vol. 3, no. 2, pp. 83–88, 2024.

[11] A. Bagir, Akhmadi, Aldrian Bachtiar Tsani, and Rafif Murti Rizky, "Penelusuran Sumber Air dan Program Mitigasi terhadap Masalah Air di Dusun Guyangan Kidul," *Jurnal Parikesit*, vol. 2, no. 1, pp. 58–65, May 2024.

[12] J. M. Putri and A. Afdal, "Identifikasi Potensi Air Tanah di Nagari Aie Dingin Menggunakan Metode Geolistrik Resistivitas," *JFU*, vol. 13, no. 1, pp. 125–131, Jan. 2024.

[13] N. A. Samudra and A. Wijaya, "Identifikasi Litologi Bawah Permukaan dengan menggunakan Metode Geolistrik Konfigurasi Schlumberger di Dusun Penimbuk, Desa Sokong, Kecamatan Tanjung, Kabupaten Lombok Barat," *JPL*, vol. 5, no. 1, p. 52, Jul. 2024.

[14] Y. Muzakki, W. Lestari, and M. H. M. Fajar, "Pemodelan Akuifer Air Tanah Menggunakan Geolistrik Resistivitas Vertical Electrical Sounding (Ves) Di Kabupaten Sorong, Provinsi Papua Barat," *jurgeo*, vol. 7, no. 3, Dec. 2021.

[15] L. Y. Irawan *et al.*, "Identifikasi karakteristik akuifer dan potensi air tanah dengan metode geolistrik konfigurasi Schlumberger di Desa Arjosari, Kecamatan Kalipare, Kabupaten Malang," *JPG*, vol. 27, no. 1, pp. 102–116, Jan. 2022.

[16] R. C. Wibowo, Suharno, Haerudin, and D. Despa, "Identifikasi Akuifer Air Tanah Menggunakan Metode Geolistrik 1 Dimensi di Kecamatan Tegineneng," *SNIP*, vol. 3, no. 1, May 2023.

[17] T. D. Syaputri, S. Suhendra, H. Halauddin, L. Lidiawati, and R. Nurhidayah, "Groundwater Study Using Vertical Electrical Sounding (VES) Data Based on Resistivity and Porosity of Rocks in Kampung Melayu, Bengkulu City," *JIS*, pp. 38–47, Apr. 2024.

[18] J. P. Sirait, M. E. Onwardana, and A. Halawa, "Identifikasi Lapisan Air Tanah Bawah Permukaan Menggunakan Metode Geolistrik Konfigurasi Schlumberger Desa Durin Tonggal, Sumatera Utara," *Jurnal Ruang Luar dan Dalam FTSP*, vol. 6, no. 2, pp. 161–166, 2024.

[19] S. E. A. Saputra, C. L. Fergusson, C. V. Murray-Wallace, and A. P. Nutman, "Neogene uplift and deformation in the northeastern Bird's Head Peninsula, West Papua, Indonesia:

consequences of oblique plate convergence," *International Geology Review*, vol. 65, no. 21, pp. 3348–3376, Nov. 2023.

[20] N. Ratman, G. Robinson, and P. Pieters, "Geological Map of the Manokwari Sheet, Irian Jaya, scale 1: 250.000," *Geological Research and Development Centre, Indonesia*, 1989.

[21] S. E. A. Saputra, C. L. Fergusson, A. Dosseto, A. Dougherty, and C. V. Murray-Wallace, "Late Quaternary neotectonics in the Bird's Head Peninsula (West Papua), Indonesia: Implications for plate motions in northwestern New Guinea, western Pacific," *Journal of Asian Earth Sciences*, vol. 236, p. 105336, Sep. 2022.

[22] A. Binley, "Tools and techniques: electrical methods," *Treatise on Geophysics*, vol. 11, pp. 233–259, Jan. 2015.

[23] B. R. Maay and J. M. Supit, "Interpretasi dan Korelasi Data Resistivitas untuk Menentukan Lapisan Akuifer Di RT.002/RW.002 Kelurahan Amban Kabupaten Manokwari Provinsi Papua Barat," *INTAN Jurnal Penelitian Tambang*, vol. 4, pp. 93–97, 2021.

[24] Kammarudin, Wahyudi, R. Lewerissa, B. Afkril, and I. S. Erari, "Groundwater Resource Estimation using Vertical Electrical Sounding and Resistivity Tomography in West Manokwari, West Papua, Indonesia," *Indonesian Physical Review*, vol. 7, no. 3, pp. 361–378, Jul. 2024.

[25] K. Pamuji, T. Tukan, and A. Musyafa, "Identifikasi Zona Akuifer Dengan Menggunakan Metode Tahanan Jenis (Resistivity) Konfigurasi Dipole-Dipole Di Kota Manokwari, Papua Barat," *Jurnal Natural*, vol. 18, pp. 13–20, May 2022.